Journal of Applied Fluid Mechanics, Vol. 9, No. 6, pp. 2969-2979, 2016.
Available online at www.jafmonline.net, ISSN 1735-3572, EISSN 1735-3645.
DOI: 10.29252/jafm.09.06.25232

Effect of Bottom Wall Heating on the Turbulent Fluid Flow in an Asymmetric Rectangular Diffuser: an Experimental Study

S. Bhattacharjee, A. Mandal†, R. Debnath, S. Majumder and D. Roy

Department of Mechanical Engineering, Jadavpur University, Kolkata-700032, West Bengal, India

†*Corresponding Author Email: arindam.mmeju@gmail.com*

(Received June 30, 2015; accepted February 1, 2016)

ABSTRACT

Turbulent fluid flow and heat transfer in an asymmetric diffuser are important in the context of the power plant engineering such as gas turbine, aircraft propulsion systems, hydraulic turbine equipment etc. In the present study, an experimental investigation on the forced convective heat transfer considering turbulent air flow in an asymmetric rectangular diffuser duct has been done. The experimental setup considered for the analysis consists of a diffuser at different bottom wall temperatures and inlet conditions. The air enters into the diffuser at a room temperature and flows steadily under turbulent conditions undergoing thermal boundary layer development within the diffuser. Efforts have been focused to determine the effects of bottom wall heating on the recirculation bubble strength, thermal boundary layer, velocity fields, temperature profiles etc. The distribution of the local average Nusselt number and skin friction factor in the whole flow fields have been critically examined to identify the significance of bottom wall heating effects on the overall heat transfer rates.

Keywords: Rectangular diffuser; Turbulent flow; Bottom wall heating; Forced convective heat transfer; Skin Friction factor; Nusselt number.

NOMENCLATURE

C_f	coefficient of skin friction	T_3	343
d	Inlet height of the diffuser	$T_{b(X)}$	bulk temperature of fluid at certain location
dt^+/dy^+	temperature gradient of the upper and lower wall of the diffuser at certain location	$T_{B,L}$	temperature at the thermal boundary layer
du/dy	velocity gradient of the upper and lower wall of the diffuser	T_{wall}, T_w	temperature of lower wall of the diffuser
g	acceleration due to gravity	u	velocity at certain location and height
Nu	average Nusselt number	u_{avg}	average velocity of fluid
Nu_x	local Nusselt number	V	center line velocity of fluid
Re	Reynolds number	Δp	difference of stagnation and static pressure
S	the distance of the station measured from the inlet end of the diffuser	ρ_{air}	density of air
T_1	absolute laboratory temperature	μ	co-efficient dynamic viscosity of fluid at room temperature
T_2	323	X	Total length of the diffuser, m

U_b	bulk average velocity	β	thermal expansion coefficient
τ_{wall}	wall shear stress	α	thermal diffusivity
k	von Kármán constant	ν	kinematic viscosity of air
Bi	additive constant	T_{in}	Inlet flow temperature
U^+	normalised mean velocity	q_{con}	average convection heat flux transferred to the fluid
y	distance from the bottom wall	h_{av}	average heat transfer coefficient of air
T^+	normalized form of temperature	k_{air}	therma conductivity of air
T	local temperature at different height at any station	Ra^*	Rayleigh number considering uniform heat flux
Gr	Grashof number	Ra	Rayleigh number

1. INTRODUCTION

In industrial applications turbulent convection flow of viscous fluids is very common phenomenon. In gas turbine engine, air is compressed in diffuser duct just upstream of the combustor. Flow separation in a diffuser causes reduction in engine performance as stated in the works of the Cherry *et al.* (2006). Obi *et al*. (1993) and Buice *et al*. (2000) thoroughly measured the mean velocity field and turbulent parameters. RANS simulation of the diffuser flow was performed by Durbin (1995) and Iaccarino (2001). A hotter plate attached with a colder stationery fluid creates a mass gradient within the domain which was explained in the works of Bejan (1993). Devia *et al*. (2000) analyzed the distribution of the heat transfer coefficient in natural convection by means of an optical technique. Numerical Analysis made by Friedrich *et al*. (2001) had shown the behaviour of the fluid subject to stable thermal stratification under the conditions of convective heat transfer in a two dimensional model. The thermal conductivity of the plexiglass side walls is much higher than that of the air as described by Lin *et al*. (1996). Incropera *et al*. (1985, 1985, 1987 and 2007) observed numerically the onset and qualitative picture of the buoyancy driven secondary flow on the bottom plate. Lewins (2004) determined the thermal boundary layer and Huang *et al*. (1996) numerically investigated the buoyancy induced transitional flow structures and heat transfer in mixed convective flow of air in a bottom heated inclined rectangular duct. Morcos *et al*. (1986) experimentally estimated the local Nusselt number while Maughan *et al*. (1987), Chang *et al*. (1998) investigated the effects of the aspect ratio on the characteristics of the longitudinal vortex air flow in a bottom heated horizontal rectangular duct by carrying out flow visualization and temperature measurement. Huang *et al*. (1995) had studied numerically the effects of Reynolds numbers on the vortex flow structure and thermal behavior in a buoyancy induced mixed convective air flow passing through a bottom heated rectangular horizontal duct. Chiu *et al*. (1987) gave the importance on the experimental processes for analysis of the flow and thermal characteristics due to the limited availability of computation process. Maughan *et al*. (1990) attempted to solve the vortex flow numerically. Lin *et al*. (1996) experimentally observed the buoyancy induced spatial and temporal flow transition and the heat transfer methods in a mixed convective steady air flow passing through a bottom heated horizontal rectangular duct. Elementary idea of buoyancy induced flow transition is important for the cooling of micro electronic equipment and transfer of heat in compact heat exchanger as discussed in the works of Incropera (1988) and Kays *et al*. (1984). Mori *et al*. (1996), Ostrach *et al*. (1975, 1976), Hwang *et al*. (1976) and Kamotani *et al*. (1979) experimentally measured the characteristics of steady longitudinal vortex rolls in a channel with bottom wall of higher uniform temperature than the top. Shuja *et al*. (1996) compared the experimental data with the numerical works and concluded that the Nusselt numbers are dependent on the Reynolds numbers. In an experimental work, Bhattacharjee *et al*. (2011) put efforts to measure the velocity profiles, pressure fields in a section perpendicular to the axis of a rectangular diffuser and at a particular diffuser angle for different inlet flow conditions. In another experimental work, Bhattacharjee *et al*. (2010) investigated the effect of two baffles of varying heights on the turbulent flow in an axi-symmetric diffuser. Recently, Majumder *et al*. (2014) have carried out an experimental study of the turbulent air flow through a rectangular diffuser using two equal baffles positioned at different axial distances from inlet of the diffuser duct. Study on the temperature gradients in the near wall region had been done by Toutant *et al*. (2013). According to the statements made by Morinishi *et al*. (2007) and Wu *et al*. (2010) the turbulent boundary layer with heat transfer remains an incompressible flow in the small temperature gradient. The mean and the turbulent profiles are considered to be asymmetric. Nicoud (1998) studied on the property variations considering a low mean Reynolds number. Serra *et al*. (2012, 2012, and 2012) realized LES parametric studies frorn different temperature ratios and Reynolds numbers. Sekimoto *et al*. (2011) stated that the mean secondary flow is driven by turbulence as well as the buoyancy in the case of thermal square-duct turbulence under the action of gravity. Ma *et al*. (2007) studied the buoyancy effects on statistics of square-duct turbulence by direct numerical simulations (DNS). The works of Kong *et al*. (2000) gave the similarity between the wall-normal heat flux and the Reynolds stresses. The theory correlates between the temperature and the

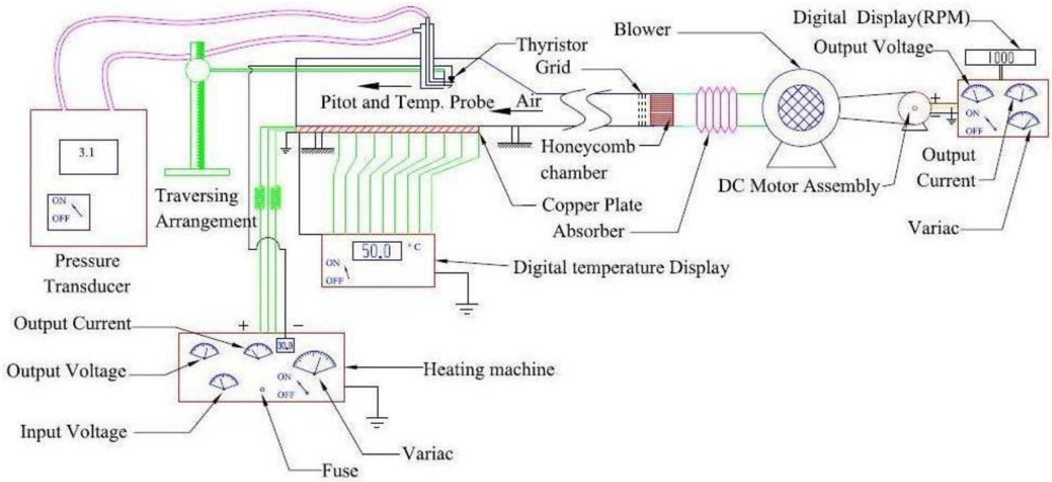

Fig. 1. Schematic view of Experimental Setup.

stream wise velocity fluctuations. Investigations on scalar transfer in turbulent channel flows at different Prandtl numbers were made by Tiselj *et al*. (2001) and Kozuka *et al*. (2009).The effect of Reynolds numbers on the scalar transfer and the variations of Prandtl numbers in channel flows were examined by Abe *et al*. (2004). Li *et al*. (2013) studied the transitional and turbulent thermal boundary layers. The studies on the scalar transport revealed the turbulent structures including the velocity and temperatures variations in flows with different thermal boundary conditions and Prandtl numbers. Recently, Zonta *et al*. (2012) examined the turbulent channel flow with wall heating by means of direct numerical simulations (DNS). They found the alteration of turbulence production and dissipation of the wall bounded flow. Lee *et al*. (2013) demonstrated the mechanism of skin-friction reduction due to the temperature dependent viscosity.

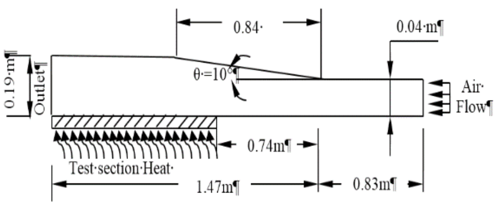

Fig. 2. Geometry of the test section.

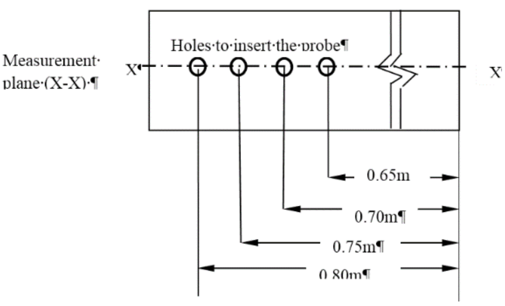

Fig. 3. Top view of the test section geometry.

In the present experimental study consideration is given on the flow characteristics and temperature measurement for turbulent forced convection flow in a rectangular diffuser. The conditions in the experimental work are taken as mixed convective steady turbulent air flow in a bottom heated horizontal rectangular diffuser. The effects of dimensionless parameters such as local Nusselt numbers and Reynolds numbers for this type of flow have been investigated.

2. EXPERIMENTAL SETUP AND MEASUREMENT TECHNIQUE

The experimental set up is schematically shown in the Fig. 1. It consists of two portions: (i) diffuser combined with air blower and power supply controller and (ii) measuring bench fitted with different apparatus for velocity and temperature. The experiment has been conducted in a rectangular diffuser of blow down type fitted with a blower. Measurements have been taken in the mid stream plane along X-X axis of Fig. 3. Air is introduced inside the diffuser by the blower over the hot copper plate and thus a velocity as well as thermal boundary layer is generated. The diffuser is a gradually diverging rectangular section of 1.47 m length (including the redevelopment channel) and the inlet cross section is 0.2 × 0.04 m. with the constant diffuser inclination angle of 10° upwards to the horizontal axis. The lower plate is made of 0.73 × 0.2 × 0.002 m of high purity rectangular copper plate heated electrically by DC power supply transferred from a variable voltage transformer. The top wall is constructed with plexiglass for better visibility. The side walls are built up with transparent glass sheet for preventing heat loss. The electrical power input is controlled by a Variac. A number of surface thermocouples (K-type made of Nickel –Aluminium) are fixed to the upper surface of the plate maintaining an interval of 0.03 m between them to measure the temperature of the copper plate at various locations. Every thermocouple is shielded against radiation. For preventing backward heat flow, insulation is provided below the copper plate. The local surface temperature of the base plate is measured by a Digital Temperature Indicator at which all the outputs of the thermocouples are connected. The measurement of heat transfer is carried out under isoflux steady state condition. The working fluid in the diffuser is air, supplied by a centrifugal type variable speed blower (Model No: DDEI-00164) fitted with a D.C. motor. A developing channel is formed which is attached with the inlet of the diffuser. The dimension of the developing section is 0.2 × 0.2 × 0.83 m. The velocities of air are measured inside the diffuser using Pitot static tube already calibrated connected with a Pressure Transducer (Range-± 10000 Pa, Air Velocity: 2 to 100 m/s). The probe made of a thyristor is used for measuring temperature of ambient air and instantaneous air temperatures at different heights inside the diffuser.

The working Newtonian fluid is air of density ρ_{air} =1.164 kg/m^3 , dynamic viscosity μ= 1.983× 10^{-5} Pa-s and kinematic viscosity of air ν= 1.7 × 10^{-5} m^2 /s at room temperature T1 = 303K and barometric pressure = 101.6 KPa. The average velocity at inlet Uav is taken as 15.308, 16.978, 22.874 m/s (Re=3.594×10^4, 3.896×10^4 and 5.371×10^4 respectively). The velocity distribution curves are obtained at different stations. The equations for the density, velocity, Reynolds numbers, Nusselt numbers, co-efficient of skin friction and the thermal boundary layer of the working fluid flowing through the diffuser are hereby given below:

$$u = \sqrt{2\Delta p \times 9.81 \big/ \rho_{air}} \qquad m/s \tag{1}$$

$$\mathrm{Re} = \rho_{air} U_b d \big/ \mu \tag{2}$$

$$Nu_x = -w\left(dt^+ / dy^+\right)_x \big/ \left[T_b(x) - T_{wall}\right] \tag{3}$$

$$\frac{T_{wall} - T_{B,L}}{T_{wall} - T_{b(X)}} = 0.99 \tag{4}$$

$$C_f = \frac{\tau_{wall}}{\left(\frac{1}{2}\right)\rho u_{avg}{}^2} = \mu \frac{du}{dy} \Big/ \frac{1}{2}\rho u_{avg}{}^2 \tag{5}$$

$U^+ = \frac{1}{k}\, ln y^+ + B_i$, where $U^+ = u_{avg}/u_*$,

$$y^+ = y\,\frac{u_*}{\nu} \text{ and } u_*^2 = \tau_{wall} / \rho_{air} \tag{6}$$

$$T^+ = T/ T_b \tag{7}$$

$$Gr = g\beta(T_w - T_{in})\, d^3/\nu^2 \tag{8}$$

$$Ra = g\beta(T_w - T_{in})\, d^3/\nu\, \alpha \tag{9}$$

$$Ra^* = g\beta q_{con}\, d^4/\nu\, \alpha\, k_{air} \tag{10}$$

$$q_{con} = h_{av}(T_w - T_{in}) \tag{11}$$

3. RESULTS AND DISCUSSIONS

Validation Study of Skin Friction Coefficient:

The experimental results shown in Fig. 4 of turbulent air flow through the asymmetric rectangular diffuser heated at the bottom horizontal wall used in the experiment have been validated with the published work of Buice *et al*. (2000) and Lan *et al*. (2009). The non dimensional value using the ratio of station distances commencing from the inlet section and height of inlet section of the diffuser are presented in the two dimensional co-ordinate system in which X-axis is parallel to the upstream flow and Y- axis is normal to the X-axis. The centre-line velocity at the inlet is 1.14U$_b$ where U$_b$ is 13.44 m/s. The Reynolds number is $\rho_{air} U_b d \big/ \mu$ or 3.594 × 10^4. The length of the settling chamber is 83 cm and the inlet height of the rectangular diffuser is 4 cm, so the ratio of the length of the settling chamber and the height of the inlet section is 20.75 which indicate the persistence of developed flow at the outlet of the diffuser. A uniform and constant heat flux is supplied at the lower horizontal wall 0.74m away from the inlet of the diffuser, the inclination angle of which is kept fixed at 10° in conformity with the set up of Buice *et al* (2000). The study is carried over at an isothermal condition at the temperature of 323K. The variations of coefficient of skin friction at different stations in the diffuser are seen with full agreement of the data provided by Buice *et al*. (2000) and Lan *et al*. (2009) which are clear from the Fig. 4. A critical observation of the skin friction profile at the section of $S/d = 10.6$, 1000 × C$_f$ = 0.059, -0.13 and -0.13 in respect of experimental, Lan *et al*. (2009) and Buice *et al*. (2000) data respectively, which shows a little difference between the experimental value with that of Lan *et al*. (2009) and Buice *et al*. (2000) data. At the station S/d= 26.25, 1000 × C$_f$ = 0.05, 0.13 and -0.13 in respect of experimental, Lan *et al* . (2009) and Buice *et al* . (2000) data respectively. At the station S/d= 30 and 37 which are at the outlet of the diffuser 1000 × C$_f$ = 0.046, 0.25, 0.84 and 0.1, 0.4,0.337 in respect of experimental, Lan *et al*. (2009) and Buice *et al*. (2000) data respectively. These phenomena explore the idea of leaning out the differences between the experimental value and the values given by Lan *et al*. [2009] and Buice *et al*. (2000). It is observed that the Skin friction coefficient distribution of present experiment and that of Buice *et al*. (2000) and Lan *et al*. (2009) is matching very well.

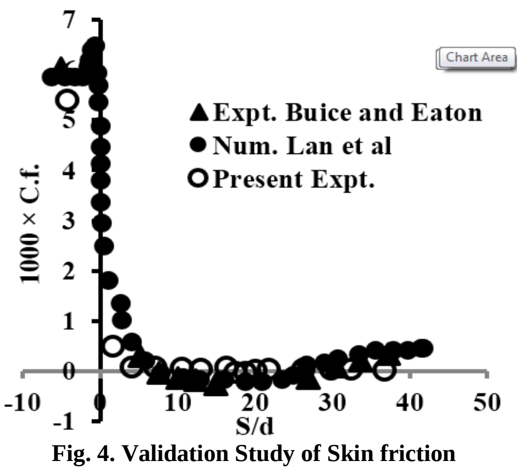

Fig. 4. Validation Study of Skin friction coefficient.

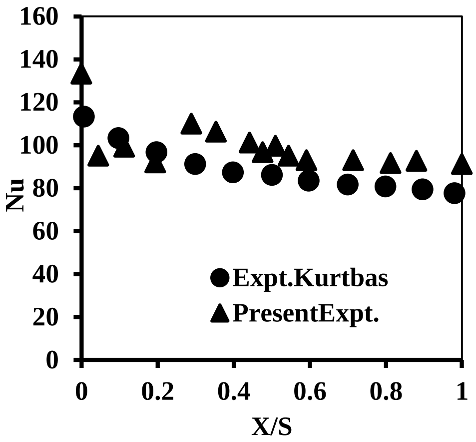

Fig. 5. Validation study of Nusselt number.

Validation Study of Nusselt Number:

The experimental study on Nusselt number distribution has been validated at Reynolds number equal to 3.594×10^4 and 343K.

At the section x/S= 0.2 away from the inlet section of the diffuser Nu=91.955 and 96.77 in respect of experimental and Kurtbas (2008) data; so the observed value is closer the value of Kurtbas (2008) data. At S/X= 0.4, 0.6, 0.8 and 1 away from the inlet section, the present experimental values of Nu become 101.2, 93.1, 91.8 and 91.3 whereas Nu data for Kurtbas (2008) are 96.77, 87.366, 83.452, 80.91 and 77.696 which also explicitly declares the good agreement between the experimental value and the published data of Kurtbas (2008). This corresponds with the other values as well.

Inlet velocities are measured for the calculation of Reynolds numbers which otherwise characterizes the nature of flow at the inlet.

The lower wall of the horizontal diffuser is heated at about $323K$ and $343K$ respectively. Measurement has been taken along the mid-stream plane $X-X$ to ensure two-dimensional flow. The velocity component at the walls equals to zero for assuming no-slip condition.

From the Fig. 6(a) to Fig. 6(c), it has been observed that there is no recirculation zone. It has been observed that velocity with the application of heat is lesser than the velocity without heating. In each of the stations the axial velocities with and without the application of heat have been estimated. Fig. 6(d) to Fig. 6(i) illustrates the recirculation zones. Fig. 6(j) to Fig. 6(l) depicts the region of reattachment of flow. Recirculation is about to start from the distance of 0.7 m measured from the inlet section of the diffuser. However recirculation does not originate from this point; it starts little earlier. Similarly it is found that flow reattachment occurs at the distance of 0.8 m away from the inlet. Here also it can be stated that reattachment appears little later. The recirculation bubble length is calculated as 0.1 m and recirculation width is 0.0225 m approximately for the case of without heating. The strength of recirculation in the case of heating decreases considerably to approximately 30-35 % reduction. Usually recirculation means a zone of low pressure with lower velocity flow reversal zone. As this zone increases, so the main flow gets shortened and the flow velocities are also changing correspondingly. So the stream wise and cross flow velocity change and simultaneously the heat transfer particularly the convective heat transfer rate also changes. This is the effect of the recirculation on the heat transfer phenomena on the opposite wall. Reynolds numbers of the inlet flows are 3.594×10^4; 3.986×10^4 and 5.371×10^4 respectively, the calculation being based on the inlet duct height and mean axial velocity. As the Reynolds number increases axial flow velocity also increases causing higher rate of heat transfer by convection. From the figures 7 (a) and (b), it is observed that coefficient of skin friction on the lower wall is decreasing faster than the upper wall. With the addition of heat, the coefficient of skin friction increases. At the recirculation zones the values of coefficient of skin friction are negative. The region of negative values of coefficient of skin friction agrees with the results under the zones of negative velocity which affirms the recirculation region. The coefficient of skin friction is estimated based on the mean velocity of air in the axial direction. The present experimental data of coefficient of skin friction over the zone of interest are correlated as the function of the Reynolds number and these correlations are valid in the Reynolds number 3.594×10^4, 3.986×10^4 and 5.371×10^4 respectively. The correlations are obtained as seen from Fig. 8(a), Fig. 8(b) and table 1.

Table 2 shows the variations of wall shear stress and skin coefficient data using log law at the wall. A minor deviation of Skin friction coefficient is occurred considering log law at the wall comparing the data with velocity gradient. Table 3 shows the dt^+/dy^+ data for evaluating Nusselt number considering logarithmic value of the normalized height and normalized temperature data at certain location (using thermal law at the wall).

Figure 9(a) and Fig. 9(b) narrate the variation of Nusselt number with the station distance measured along the axial direction in the mid-stream plane $\mathbf{X}-\mathbf{X}$. At the thermally developing region of flow which starts from the distance 0.74 m away from the inlet section of the diffuser Nusselt number increases showing greater amount of heat transfer by convection and thereafter it becomes nearly constant at the downstream of the diffuser. This is because the thermal boundary layer is simultaneously developing along with the velocity boundary layer. When the thermal Boundary Layer gets fully developed then the temperature gradient becomes zero. So the Nusselt number practically becomes constant. Towards the downstream side of the diffuser the difference between the surface temperature and ambient temperature becomes larger causing Nusselt number to decrease.

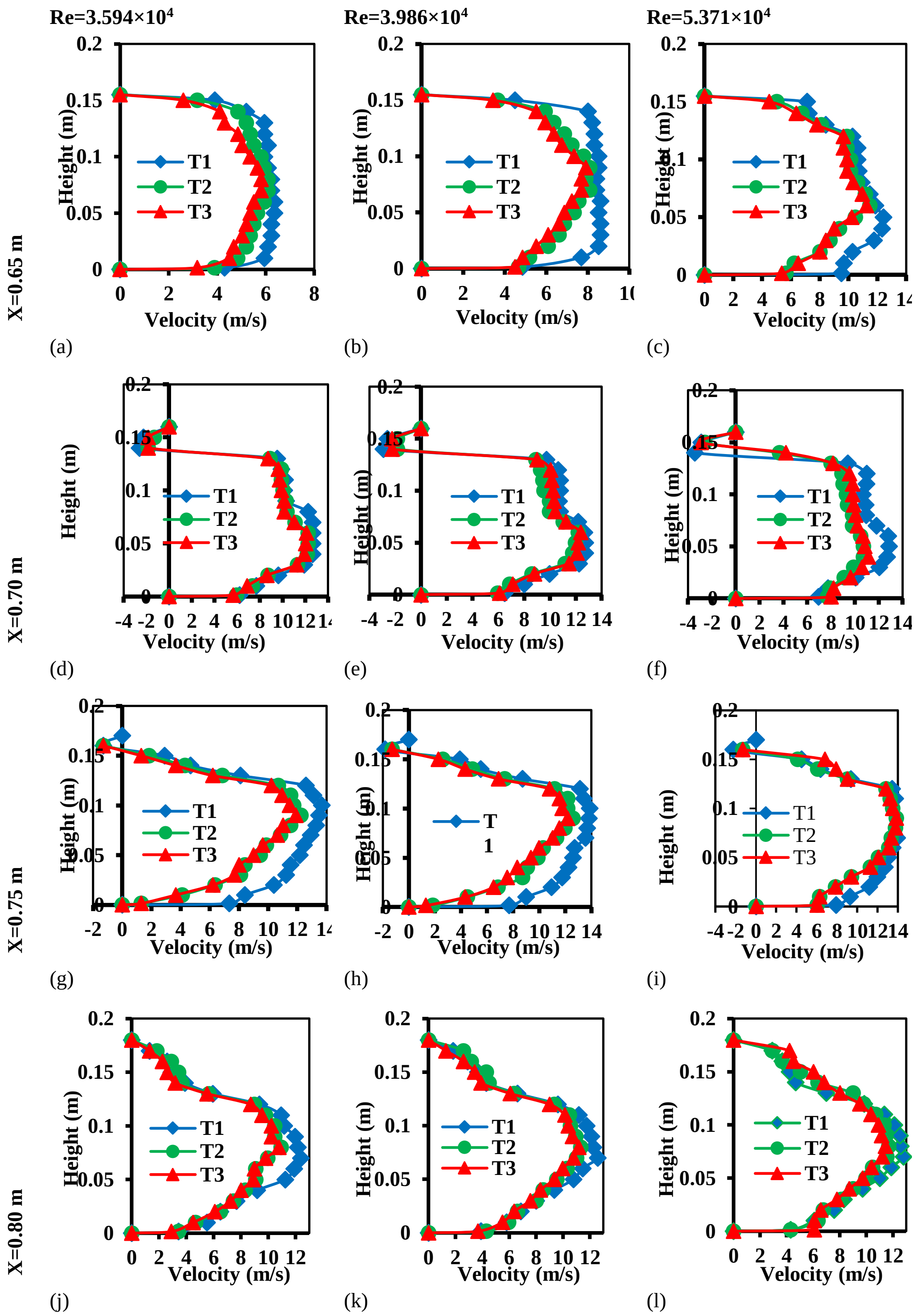

Fig. 6. Axial Velocity profile at different location.

Table 1 Correlation between C_f and Re

Thermal Condition	C_f at Lower wall	C_f at Upper wall
Without heating	$0.631Re^{-0.71}$	$1.504Re^{-0.91}$
$323K$	$0.191Re^{-0.59}$	$2.14Re^{-0.94}$
$343K$	$0.006Re^{-0.27}$	$10.92Re^{-1.09}$

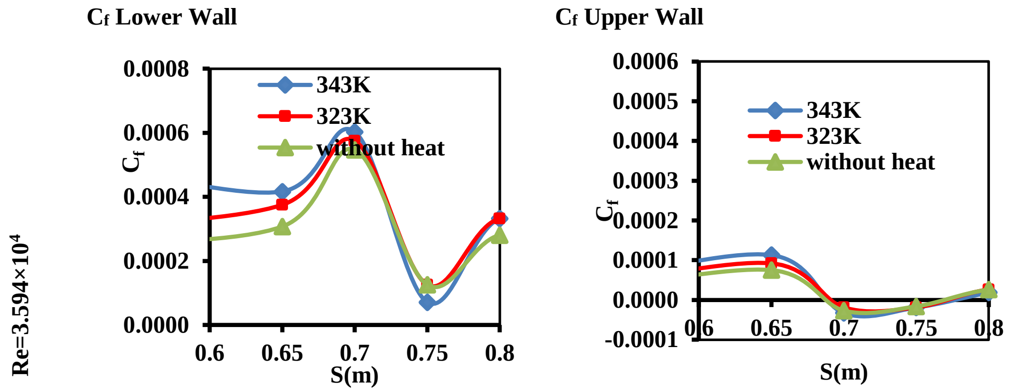

(a) (b)

Fig. 7. Coefficient of Skin Friction.

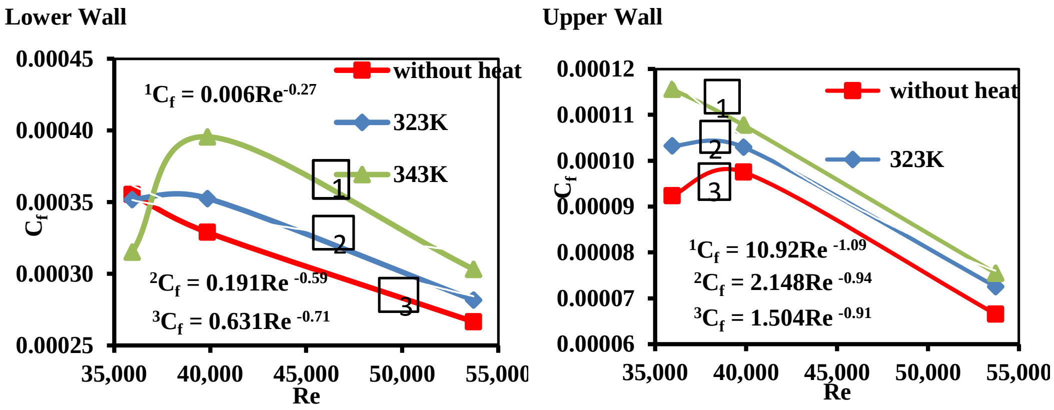

(a) (b)

Fig. 8. Variation of Coefficient of skin friction with Reynolds Number.

Table 2 τ_{wall} and C_f using log law at the wall

	C_f (Lower wall)	τ_{wall} (Lower wall)	Stations, m	τ_{wall} (Upper wall)	C_f (Upper wall)
Re=3.594× 10^4	6.87× 10^{-4}	9.36× 10^{-2}	S=0.65	5.72 × 10^{-2}	4.19× 10^{-4}
			S=0.7& 0.75	-3.41× 10^{-2}	-2.50× 10^{-4}
			S=0.8	3.41× 10^{-2}	2.50× 10^{-4}
Re=3.986× 10^4	5.16× 10^{-4}	8.65× 10^{-2}	S=0.65	5.74× 10^{-2}	3.42× 10^{-4}
			S=0.7& 0.75	-3.14× 10^{-2}	-1.87× 10^{-4}
			S=0.8	3.14× 10^{-2}	1.87× 10^{-4}
Re=5.371× 10^4	2.31× 10^{-4}	7.04× 10^{-2}	S=0.65	4.23× 10^{-2}	1.39× 10^{-4}
			S=0.7& 0.75	-2.51× 10^{-2}	-8.23× 10^{-4}
			S=0.8	2.51× 10^{-2}	8.24× 10^{-4}

Table 3 dT^+/dY^+ using log law at the wall

	Stations, m	Re=3.594× 10^4	Re=3.986× 10^4	Re=5.371× 10^4
323K	0.65	0.545031	0.515962	0.487445
	0.7	0.562358	0.531349	0.502414
	0.75	0.580587	0.541385	0.505873
	0.8	0.577511	0.538524	0.507023
343K	0.65	0.544071	0.515121	0.487285
	0.7	0.54552	0.51511	0.487141
	0.75	0.545973	0.515263	0.48804
	0.8	0.545823	0.518063	0.490763

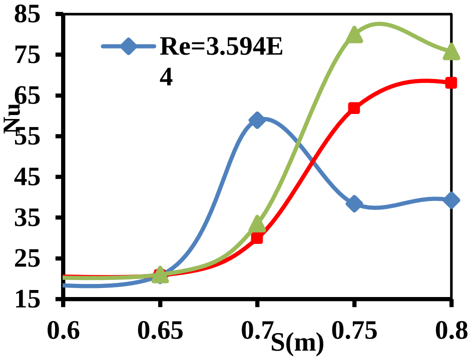

Fig. 9. (a) Nusselt number variation along the lower wall at 323K.

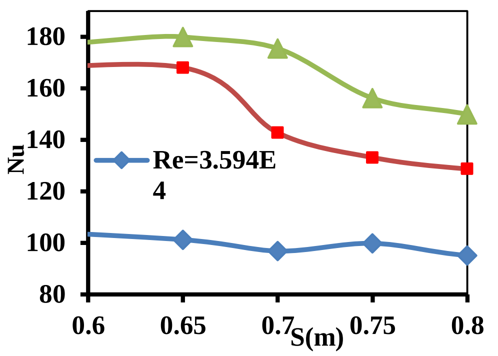

Fig. 9. (b) Nusselt number variation along the lower wall at 343K.

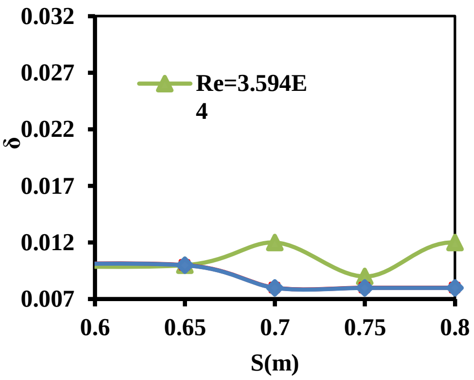

Fig. 10. (a) Thermal Boundary Layer at 323K.

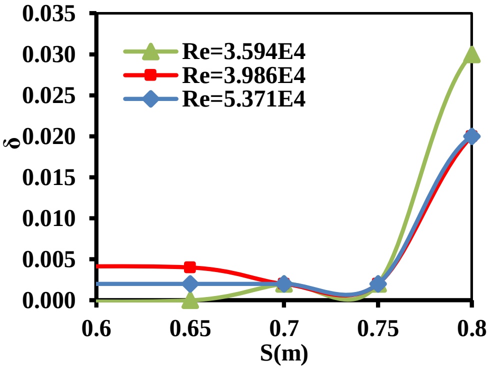

Fig. 10. (b) Thermal Boundary Layer at 343K.

Table 4 q_{con} at different locations

	Stations, m	Re=3.594× 10^4	Re=3.986× 10^4	Re=5.371× 10^4
323K	0.65	200	120	50
	0.70	900	500	300
	0.75	2000	2000	2000
	0.80	2000	2000	2000
343K	0.65	500	300	100
	0.70	1200	1200	500
	0.75	4000	4000	4000
	0.80	4000	4000	4000

From Fig. 11 it is observed that with the increase of Reynolds number average Nusselt number increases due to the large forced convection of heat flow and turbulence of air. The average Nusselt number is estimated by integrating the local Nusselt numbers. From the experimental observation the correlations between average Nusselt numbers and Reynolds numbers for the air flow inside a diffuser are obtained at the temperatures $323K$ and $343K$ as per the table 5. Table 4 shows the variation of average convection heat flux transferred to the air considering h_{av} = 100 W/m^{2}K .

The above mentioned correlations are valid for Reynolds numbers 3.594×10^4, 3.986×10^4 and 5.371×10^4 respectively. Figs. 10(a) and 10(b) represent the thermal boundary layer profiles with respect to the axial distances at the temperatures $323K$ and $343K$ respectively. Thermal Boundary layer fluctuates more as the heated plate is approached. Fluctuation increases with the increase of temperature. As Reynolds number increases the thickness of Thermal Boundary Layer decreases. At the outlet of the diffuser the thickness becomes nearly constant.

From the graphical interpretation of Fig. 6(d) and Fig. 6 (e) it has been noticed that the velocity with heating is little more than without heating. This discrepancy is not abrupt since the recirculation has been found to be preceded little earlier for the case of without heating. So it is expected that the recirculation followed by the flow separation for the case of without heating will be terminating or the reattachment point will be shifted further downstream for the case of with heating.

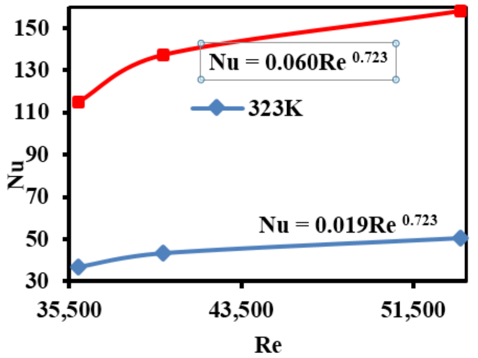

Fig. 11 Variation of Nusselt number with Reynolds number.

Table 5 Correlation between Nusselt Number with Re

Thermal Condition	Nusselt Number
323K	$Nu=0.019Re^{0.723}$
343K	$Nu=0.06Re^{0.723}$

Table 6 Gr and Ra at different temperatures

	323K	343K
Gr	1.44×10^5	2.88×10^5
Ra	20928	41856
Ra^*	3.17×10^6	6.34×10^6

A major finding of the research work is whether the recirculation increases, remains constant or decreases for bottom wall heating. The present researcher found that the recirculation decreases with the increase of temperatures. This can be attributed due to the reason that the heating results in increase of viscosity and lowers the flow velocity. The augmented viscous effects are dominant particularly near the wall and this is responsible for this phenomenon. A higher velocity is quite capable of withstanding the adverse pressure gradient further downstream rather than a lower flow velocity, which is prone to separate due to inability to counter an adverse pressure gradient earlier. The ultimate consequence is the reduction of the recirculation bubble strength for the case of application of heat to the flow from the lower wall.

4. DISCUSSION ON GRASHOF NUMBER AND RAYLEIGH NUMBER

Buoyancy and viscous forces in the fluid influences the transition in a free convection boundary layer. Grashof number is calculated as 2.88×10^5 whereas Rayleigh number is equal to 20928 and 41856 considering the bottom wall temperature as 323K and 343K. When uniform heat flux is considered Rayleigh number changes to 3.17×10^6 and 6.34×10^6 at the same conditions. Here thermal diffusivity $\alpha = 1.17 \times 10^{-4}$ m^2 /s , $\beta = 3.315 \times 10^{-3}$ (1/K) and k_{air} = 0.0264 W/mK.

A greater value of Rayleigh number significantly describes the heat transferred by the convection method from the bottom most wall to the upper surface and consequently, the flow becomes turbulent.

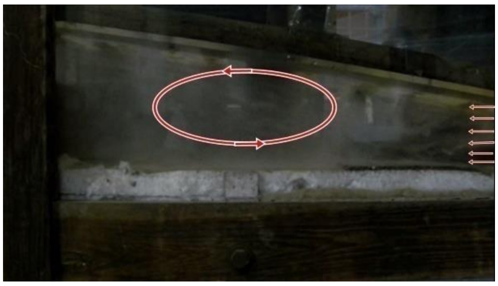

Fig. 12. Visualisation Study.

5. VISUALISATION STUDY

A high resolution camera is used for taking the photograph and white smoke is used as the indicator delivered from the inlet section of the diffuser. From the visualization study indicated by the red marking it has been seen that recirculation starts on the upper inclined wall at the upstream section of the diffuser and gets diminished at the downstream portion. The size of the recirculation bubble is nearly same as determined by the experimental process. With the application of heat the recirculation regime becomes somewhat decreased.

6. CONCLUSIONS

- Forced convective heat transfer inside a two dimensional rectangular asymmetric (10o axial inclination) with bottom wall horizontal diffuser is investigated experimentally. The experiment has been carried out under a uniform wall heat flux within of Reynolds numbers 3.594×10^4, 3.986×10^4 and 5.371×10^4 and temperatures of $323K$ and $343K$ respectively.
- The recirculation is generating at the upper wall of the diffuser. Before and after the recirculation the velocity profiles are turbulent like distributions.
- With the application of heat recirculation strengths reduce appreciably.
- With the increase of Reynolds number the value of coefficient of friction increases.
- With the increase of Reynolds number, Nusselt number increases exhibiting more enhancement of heat transfer. The Nusselt number is more for higher temperature.
- Empirical correlations are established for the Average Nusselt number and coefficient of

friction with Reynolds number which can be roughly used for the estimation of these quantities.

ACKNOWLEDGEMENT

The authors express their sincere thanks and gratitude to all who are extending their helping hand by giving valuable suggestions and technical support for this work done at Hydraulics Laboratory, Mechanical Engineering Department, Jadavpur University, Kolkata (India).

The author[2] also acknowledges the financial support of UGC (RGNF), Govt. of India.

REFERENCES

Abe, H., H. Kawamura and Y. Matsuo (2004). Surface heat-flux fluctuations in a turbulent channel flow up to $Re_\tau = 1020$ with $Pr = 0.025$ and 0.71. *Int. J. Heat and Fluid Flow* 25, 404-419.

Bejan, A. (1993*). Heat Transfer*, John Wiley and Sons, New York.

Bhattacharjee, S., R. Debnath, A. Mandal, D. Roy and S. Majumder (2010). Experimental investigation of Recirculatory turbulent flow past twin obstructions of different heights placed at different stations of a Rectangular diffuser. In *Proceedings of the 37th National and 4th International Conference on Fluid Mechanics and Fluid Power*, IIT Madras, Chennai, India, EM – 05, 1-8.

Bhattacharjee, S., R. Debnath, D. Roy and S. Majumder (2011). An experimental study on turbulent air flow through a two-dimensional rectangular diffuser. *IE (I) Journal-MC* 92, 3-7.

Buice, C. U. and J. K. Eaton (2000). Experimental Investigation of Flow through an Asymmetric Plane Diffuser. *Journal of Fluid Engineering* 122, 433-435.

Chang, M. Y. and T. F. Lin (1998). Experimental study of aspect ratio effects on longitudinal vortex flow in mixed convection of air in a horizontal rectangular duct. *Int. J. Mass Transfer* 41, 719-733.

Cherry, E. M., G. Iaccarino, C. J. Elkins and J. K. Eaton (2006). Separated flow in a three dimensional diffuser: preliminary validation. *Annual Research Briefs, Center for Turbulence Research* 31-40.

Chiu, K. C., J. Quazzani and F. Rosenberger (1987). Mixed convection between horizontal plates-II. Fully developed flow. *Int. J. Heat Mass Transfer* 30, 1655-1662.

Devia, F. and G. Tanda (2000). Investigation of natural convection heat transfer from a horizontal isothermal plate by Schlieren tomography. *Int. J. Heat Technology* 18, 41-46.

Durbin, P. (1995). Separated Flow Computations with the k-ε-v^2 Model. *AIAA Journal* 33, 659-664.

Friedrich, M. K. and D. Angirasa (2001). Interaction between stable thermal stratification and convection under a heated horizontal surface facing downwards. *Int. J. Non-Linear Mech.* 36, 719-729.

Huang, C. C. and T. F. Lin (1996). Numerical simulation of transitional aiding mixed convective air flow in a bottom heated inclined rectangular duct. *Int. J. Heat Transfer* 39, 1697-1710.

Huang, C. C. and T. F. Lin (1995). Vortex flow and thermal characteristics in mixed convection of air in a horizontal rectangular duct: effects of the Reynolds and Grashof numbers. *Int. J. Heat Mass Transfer* 38(1), 661-1674.

Hwang, G. J. and C. L. Liu (1976). An experimental study of convective instability in the thermal entrance region of a horizontal parallel-plate channel heated from below. *Canadian Journal of Chemical Engineering* 54, 521-525.

Iaccarino, G. (2001). Prediction of a turbulent separated flow using commercial CFD codes. *Journal of Fluids Engineering* 123, 819-828.

Incropera, F. P., D. P. Dewitt, T. Bergman and A. Lavine (2007). *Fundamentals of Heat and Mass Transfer*, 6th Ed., Wiley.

Incropera, F. P. (1988). Convective heat transfer in electronic equipment cooling. *J. Heat Transfer* 110, 1097-1111.

Incropera, F. P. and D. G. Osborne (1985). Experimental study of mixed convection heat transfer for transitional and turbulent flow between horizontal, parallel plates. *Int. J. Heat Mass Transfer* 28, 1337-1344.

Incropera, F. P. and D. G. Osborne (1985). Laminar, mixed convection heat transfer for flow between horizontal parallel plates with asymmetric heating. *Int. J. Heat Mass Transfer* 28, 207-217.

Incropera, F. P., A. L. Knox and. J. R. Maughan (1987). Mixed convection flow and heat transfer in the entry region of a horizontal rectangular duct. *J. Heat Transfer* 109, 434-439.

Kamotani, Y., S. Ostrach and H. Miao (1979). Convective heat transfer augmentation in thermal entrance regions by means of thermal instability. *Journal of Heat Transfer* 101, 222-226.

Kays, W. M. and A. L. London (1984*). Compact Heat Exchangers*, 3rd. Ed., McGraw-Hill New York.

Kong, H., H. Choi and J. S. Lee (2000). Direct numerical simulation of turbulent thermal boundary layers. *Physics of Fluids* 12, 2555-2568.

Kozuka, M., Y. Seki and H. Kawamura (2009). DNS of turbulent heat transfer in a channel flow with a high spatial resolution. *Int. J. Heat and Fluid Flow* 30, 514-524.

Kurtbas, I. (2008). The effect of different inlet conditions of air in a rectangular channel on convection heat transfer: Turbulence flow. Expt. *Thermal and fluid Science* 33, 140-152.

Lan, H., B. F. Armaly and J. A. Drallmeier (2009). Turbulent Forced Convection in a Plane Asymmetric Diffuser: Effect of Diffuser Angle. *J. Heat Transfer, Trans. ASME* 131

Lee, J., S. Y. Jung, H. I. Sung and T. A. Zaki (2013). Effect of wall heating on turbulent boundary layers with temperature-dependent viscosity. *J. Fluid Mech*. 726, 196-225.

Lewins, J. D. (2004). Comparative solutions to the integral approximate thermal boundary layer equations for a flat plate. *Int. J. Mechanical Engineering Education* 32, 315-344.

Li, Q., P. Schlatter, L. Brandt and D. S. Hennigson (2013). DNS of a spatially developing turbulent boundary layer with passive scalar transport. *Int. J. Heat and Fluid Flow* 30, 916-929.

Lin, W. L. and T. F. Lin (1996). Experimental study of unstable mixed convection of air in a bottom heated horizontal rectangular duct. *Int. J. Heat Mass Transfer* 39, 1649-1663.

Lin, W. L., Y. T. Ker and T. F. Lin (1996). Experimental observation and conjugated heat transfer analysis of vortex flow development in mixed convection of air in a horizontal rectangular duct. *Int. J. Heat and Mass Transfer* 39, 3667-3683.

Ma, L. D., Z. Y. Li and W. Q. Tao (2007). Direct numerical simulation of turbulent flow and heat transfer in a square duct with natural convection. *Heat Mass Transfer* 44, 229-250.

Majumder, S., D. Roy, S. Bhattacharjee and R. Debnath (2014). Experimental investigation of the turbulent fluid flow through a rectangular diffuser using two equal baffles. *J. Inst. Eng. India Ser. C* 95, 19-23.

Maughan, J. R. and E. P, Incropera (1990). Fully developed mixed convection in a horizontal channel heated uniformly from above and below. *Numerical Heat Transfer* 17, 417-430.

Maughan, J. R. and F. P. Incropera (1987). Experiments on mixed convection heat transfer for air flow in a horizontal and inclined channel. *Int. J. Heat Transfer* 30, 1307-1318.

Morcos, S. M., M. M. Hilal, M. M. Kamel and M. S. Soliman (1986). Experimental investigation of mixed laminar convection in the entrance region of inclined rectangular channels. *Int. J. Heat Mass Transfer* 108, 574-579.

Mori, Y. and Y. Uchida (1996). Forced convective heat transfer between horizontal flat plates. *Int. Journal of Heat & Mass Transfer* 9, 803-817.

Morinishi, Y., S. Tamano and E. Nakamura (2007). New scaling of turbulence statistics for incompressible thermal channel flow with different total heat flux gradients. *International J. of Heat and Mass Transfer* 50, 1781-1789.

Nicoud, F. C. (1998). Numerical Study of a Channel Flow with Variable Properties. Center for turbulent Research. *Annual Research Briefs* 289-309.

Obi, S., K. Aoki and S. Masuda (1993). Experimental and Computational Study of Separating Flow in an Asymmetric Plane Diffuser. *9th Symposium on Turbulent Shear Flows*, Kyoto, Japan, 1-4.

Ostrach, S. and Y. Kamotani (1975). Heat transfer augmentation in laminar fully developed flow by means of heating from below. *Journal of Heat Transfer* 97, 220-225.

Ostrach, S. and Y. Kamotani (1976). Effect of thermal instability of thermally developing channel flow. *Journal of Heat Transfer* 98, 62-66.

Sekimoto, A., G. Kawahara, M. Sekiyama and A. Pinelli (2011). Turbulence and buoyancy driven secondary flow in a horizontal square duct heated from below. *Physics of Fluids* 23.

Serra, S., A. Toutant and F. Bataille (2012). Thermal Large eddy simulation in very simplified geometry of a solar receiver. *Heat Transfer Engineering* 33, 505-524.

Serra, S., A. Toutant, F. Bataille and Y. Zhou (2012). Turbulent kinetic energy spectrum in very anisothermal flows. *Physics Letters, A* 376, 3177-3184.

Serra, S., A. Toutant, F. Bataille and Y. Zhou (2012). High-temperature gradient effect on a turbulent channel flow using thermal large-Eddy simulation in physical and spectral spaces. *J. of Turbulence* 13, 1-25.

Shuja, S. Z. and M. A. Habib (1996). Fluid flow and heat transfer characteristics in axisymmetric annular diffusers. *Computers & Fluids* 25, 133-150.

Tiselj, I., E. Pogrebnyak, C. Li, A. Mosyak and G. Hetsroni (2001). Effect of wall boundary condition on scalar transfer in a fully developed turbulent flume. *Physics of Fluids* 13, 1028-1039.

Toutant, A. and F. Bataille (2013). Turbulence statistics in a fully developed channel flow submitted to a high temperature gradient. *International Journal of Thermal Sciences* 74, 104-118.

Wu, X. and P. Moin (2010). Transitional and turbulent boundary layer with heat transfer. *Physics of Fluids* 22.

Zonta, F., C. Marchioli and A. Soldati (2012). Modulation of turbulence in forced convection by temperature-dependent viscosity. *J. Fluid Mech.* 697, 150-174.